Polym. Bull. (2009) 62:791–800
DOI 10.1007/s00289-009-0051-1

ORIGINAL PAPER

Properties of polyamide 6/clay nanocomposites processed by low cost bentonite and different organic modifiers

D. García-López · I. Gobernado-Mitre · J. F. Fernández · J. C. Merino · J. M. Pastor

Received: 11 April 2008 / Revised: 18 July 2008 / Accepted: 10 February 2009 /
Published online: 19 February 2009

Abstract Nanocomposites based on polyamide 6 have been directly prepared by melt compounding, using modified low cost bentonites by three selected quaternary ammonium cations, in particular quaternized octadecylamine (ODA), dimethyl benzyl hydrogenated tallow quaternary ammonium (B2MTH) and dimethyl hydrogenated ditallow quaternary ammonium (2M2TH). Thermal stability of organic modifiers and organoclays has been studied by TGA and results allow evaluating the degree of modifier incorporation into clay galleries. The influence of the organic modifier on the morphology and properties of the obtained nanocomposites has been studied by X-ray diffraction and TEM analysis. Depending on the degree of bentonite modification, different mechanisms were reported to explain the improved mechanical properties of the resulting nanocomposites.

Keywords Nanocomposites · Polyamide 6 · Organic modifier · Bentonite · Melt compounding

D. García-López (✉) · I. Gobernado-Mitre · J. C. Merino · J. M. Pastor
Center for Automotive Research and Development (CIDAUT),
Technological Park of Boecillo, 47151 Valladolid, Spain
e-mail: garlop@cidaut.es

J. F. Fernández
Electroceramic Department, Instituto de Cerámica y Vidrio, CSIC. Kelsen 5,
28049 Madrid, Spain

J. C. Merino · J. M. Pastor
Dpto. Física de la Materia Condensada,
E.T.S.I.I. Universidad de Valladolid, 47011 Valladolid, Spain

Introduction

Polymer layered silicate nanocomposites based on thermoplastic polymers usually display significant improvements in modulus and heat deflection temperature at relatively low levels of reinforcement (3–8% wt). Other properties as permeability and retardant enhancements with respect to the unmodified polymers are also improved [1]. The vast majority of the work in nanocomposites has been focussed on the use of montmorillonite type clays as nanoparticles. The mechanical properties of the nanocomposites are strongly dependent on the degree of exfoliation and dispersion of the bentonite aggregates in the polymer matrix. The most pronounced changes in nanocomposite morphology as well as mechanical properties result from altering the number and types of groups or tails attached to the nitrogen atom of the modifier compound. Paul et al. [2, 3] found a significant influence of the long alkyl groups on the exfoliation level. They show that a most effective exfoliation is obtained with an organoclay having one alkyl tail in the quaternary cation. On the other hand, Limpanart et al. [4] have found that the surface coverage of the organoclay play a major role in controlling the type of the final composite formation in Polystyrene-clay nanocomposites.

Once the organoclay is obtained, it may be added to the monomer before the polymerization stage [5, 6] or directly to the polymeric matrix in a melt mixing process [7] to produce the nanocomposite material. We have recently obtained [8] that an excess of organic modifier negatively affects the properties of the melt compounded nanocomposite. The thermal stability of the organic modifier is related to the groups linked to the quaternary ammonium, and it must be previously checked that the organic modifier is not decomposed during the compounding process. Thus, modifier compounds should not only produce the exfoliation of the clays but also remain thermally stable during the compounding process if in principle the processing temperature is below the modifier decomposition temperature.

The aim of this work is to compare the morphology and mechanical properties of melt processed polyamide 6/layered-silicate nanocomposites based on different organoclays by using a low cost bentonite raw material.

Experimental

Materials

The polymeric material used for the preparation of polyamide 6 nanocomposites was a commercial PA 6 (Bergamid B 90, PolyOne); this matrix was characterised to have a high viscosity. The clay raw material kindly supplied by Tolsa S.A. (Spain) was sodium bentonite type clay with the following mineralogical composition (dry% wt): 63 montmorillonite, 18 dolomite, 10 illite, 4 quartz, 3 calcite and 2 paglioclase. The purification process was previously described [8] and allows using this clay having a cation exchange capacity (CEC) of 80 meq/100 g. The organic modifiers were: octadecylamine (ODA), dimethyl benzyl hydrogenated tallow

quaternary ammonium (modified B2MTH) and dimethyl hydrogenated ditallow quaternary ammonium (modified 2M2TH), where hydrogenated tallow (HT) is ~65% of C18; ~30% C16; ~5% C14. ODA with a molecular weight of 269 mol/g was supplied from Aldrich with a purity >90%. Commercial B2MTH and 2M2TH were supplied by KAO with a purity of >75 and >85%, respectively. Molecular weights were 415 mol/g for B2MTH and 570 mol/g for 2M2TH.

The preparation method of the organophilic bentonite clays was also described in a previous paper [8].

The nanocomposites were elaborated through an extrusion process using a Leistritz 27 GL intermeshing twin screw extruder operating at 240–250 °C and 450 rpm in corrotating mode. The polymer matrix was added through the first feeder and the clay through a side feeder. PA 6 granulates were dried at 80 °C for 8 h, and the modified clay was dried at 60 °C for 24 h prior to blending in the extruder. After being dried at 80 °C for 8 h, pellets of the nanocomposites were injection moulded into test pieces for mechanical tests by using a Margarite JSW110 injection moulder. The temperature of the cylinders was 240–250 °C and that of the mould was 80 °C.

Characterisation

The morphology of the modified bentonites and nanocomposite fracture were studied by using a field emission scanning electron microscope (FESEM) Hitachi S4700 after gold coating. The gallery distance of the clays was evaluated by measuring the d_{001} X-ray reflection in a Philips X'Pert MPD using Cu Kαradiation. The dispersion of the silicate layers in the polymers was evaluated in ultrathin section by using Transmission Electron Microscopy (TEM) Jeol JEM 2000FX Electron Microscope with 200 kV accelerating voltage. Mechanical properties were evaluated using an Instron tester (Model 5500R60025) according to UNE-EN ISO 527-1 and 527-2. Heat deflection temperature (HDT) was measured in an HDT-VICAT tester microprocessor, ATS-FAAR (Model A/3M) according UNE-EN ISO 75-1 and using a load of 1.8 MPa. For Notched Izod impact strength a pendulum trademark Frank Model 53566 was used under UNE-EN ISO 180. Thermal stability of the organoclays and clay contents in the nanocomposites were measured by burning the samples in a Thermogravimetry Analysis Mettler Toledo Model TGA851.

Results and discussion

The TG and DTG curves obtained for the modified bentonites are shown in Fig. 1 and Table 1 presents the percent weight loss. The thermal decomposition of these nanoclays fits a four-step mechanism. Volatilization of the water molecules adsorbed on the clays is first detected (~60 °C) and a further degradation of inorganic crystallised water molecules is detected at 800 °C. Degradation steps at 200–450 °C are associated with the organic modifiers [8]. The decomposition processes that take place between 150 and 350 °C may be related to free modifier

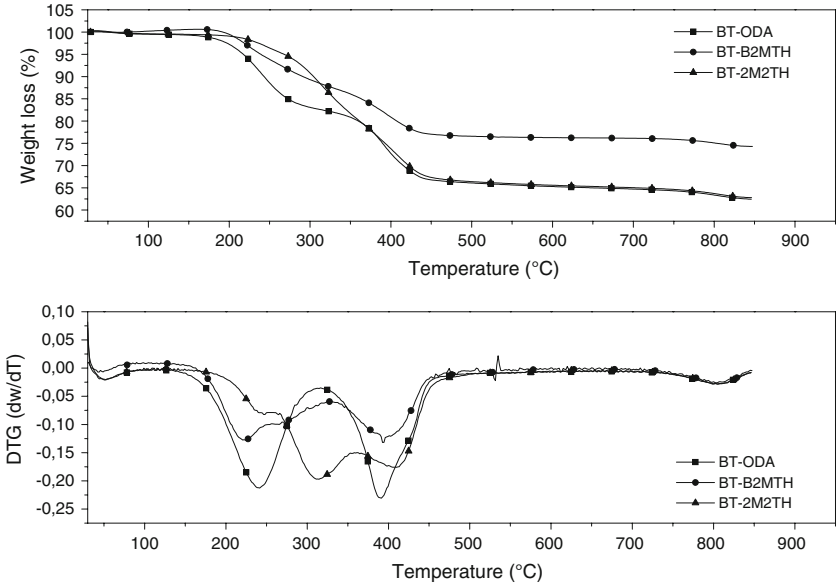

Fig. 1 TG and DTG curves of the organoclays

Table 1 Thermogravimetric analysis values of organoclays

Organoclay	25–100 °C		150–350 °C		350–500 °C		750–850 °C		Organic modifier (%)
	Mass (%)	T (°C)	Mass (%)	T (°C)	Mass (%)	T (°C)	Mass (%)	T (°C)	
BT-ODA	0.77	59	16.85	238	16.84	394	2.41	790	33.68
BT-B2MTH	0.83	57	15.18	251	12.73	398	2.23	798	27.91
BT-2M2TH	0.70	59	20.41	308	13.29	408	1.95	799	33.70

Temperature values were measured on the mid-point of the curve that corresponds to the decomposition of the 50 wt% of the compound

and the modifier that is adsorbed on microfiller, and the degradation of the organic modifier that is located in the clay galleries is detected at 350–500 °C. In this sense, whereas for both ODA and B2MTH thermal stability is considerably increased when they are interacting with the clay, a less significant increase was detected for 2M2TH. However, the decomposition temperature of the modifiers into the galleries reached a quite similar temperature range, and therefore the increase in the decomposition temperature should be related to the chemical bonding of the alkyl tallow chains into the galleries of the inorganic layered silicates.

Considering that the weight loss detected between 350 and 500 °C corresponds exclusively to the modifier that is located into the clay galleries, it is possible to establish a ratio between the effectively incorporated organic modifier and the CEC of the clay. The CEC must account for the available sites in the layered silicate.

Thus, we define this ratio as gallery effective modifier, R_{gem} = modifier into the galleries/stoichiometric modifier required. For the nanoclays under study this R_{gem} ratio was 0.95, 0.51 and 0.42 for ODA, B2MTH and 2M2TH, respectively. Therefore, the higher the modifier molecular weight, the lower the incorporation to the clay galleries. The increase of the amount of alkyl tails has a similar effect due to their high stereochemical nature. The modifier that is not incorporated into the clay galleries is probably adsorbed on the clay surface or on the impurity surfaces. The decomposition temperature established the presence of modifier at the surface and no other proofs until now were support such hypothesis. The decreasing of the decomposition temperature in reference to the free modifier is thus attributed to a catalyst effect of the clay surface. Possible interaction of the modifier with clay surface must be occur through the surface hydroxyl groups resulting in a different bounding than the one that may occurs in the galleries trough the basal oxygen of the silica tetrahedral. It is important to remark that the total amount of modifier is very similar in the nanoclays BT-ODA and BT-2M2TH, $\sim$33.7% wt, but the R_{gem} was almost double for the first one because of the higher effectiveness of low molecular weight modifier.

In Fig. 2a, the small angle X-ray diffraction (SAXD) patterns of the unmodified and modified bentonites are shown. The treatment of clays resulted in intercalation of the organic modifiers between the clay galleries, and thus a shift in the peaks to lower 2θ values is detected. The different increases in basal spacing indicate that the interchange between the alkaline ions and the organic modifiers in the clays galleries has a different extension and efficiency. The starting bentonite clay has an interlayer of 1.21 nm that indicated the hydration process of the galleries because of the purification process. For BT-ODA the presence of unmodified bentonite was almost not detected, which is in accordance to their higher R_{gem} ratio that represent a high amount of modifier into the clay galleries as measured by TGA, whereas a significant amount of unmodified clay was detected for BT-2M2TH and BT-B2MTH. On the other hand, BT-ODA XRD pattern shows two distinct peaks, which reflects the presence of modifier intercalated into the clay galleries in structures that gave a thicker interlayer space than the monolayer structure as can be account for bimodal lamellar structure and paraffinic structure [9, 10]. B2MTH and 2M2TH organoclays present a dissimilar behaviour probably due to the different molecular structure of the organic modifiers. As higher the molecular weight higher the interlayer space. Moreover, the presence of two alkyl tails shows a gradually increase of the interlayer space with a less defined peak associated with a wider distribution of interlayer spaces.

The X-ray diffraction patterns for the nanocomposites obtained by melt compounding of PA6 and organoclays are shown in Fig. 2b. Similar gallery distances are detected for the three nanocomposites, although a slight higher value (3.46 nm) is detected for the nanocomposite with BT-2M2TH, indicating a higher degree of intercalation of the polymeric chains into the clay galleries. The exfoliation level for all the nanocomposites is difficult to measure by XRD but in this case the presence of a peak at 8.9° that correspond to a fibrillar morphology illite mineral indicates that the amount of non-swellable layered clay was almost negligible. Note that this peak was also present in the raw material with very low

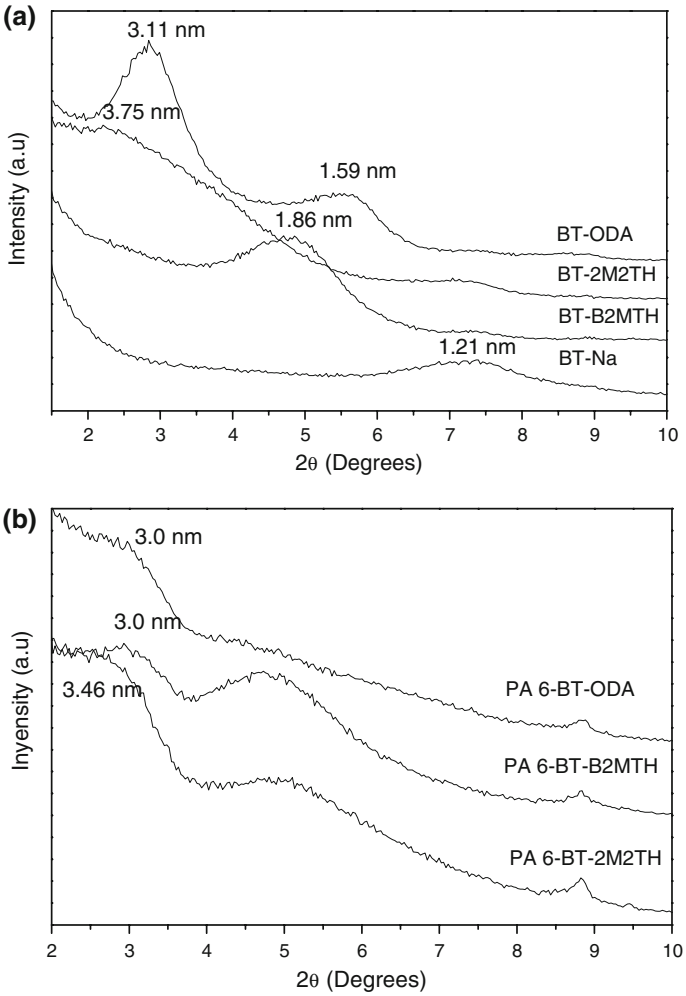

Fig. 2 XRD patterns of **a** the organoclays and **b** the PA 6 nanocomposites

intensity (Fig. 2a). However, the presence of a broad peak at 2 nm for PA-BT-2M2TH indicated that a higher interlayer gallery collapses without intercalation of polymeric chains. By the contrary for the PA-BT-B2MTH there is an increase of the interlayer distance from 1.86 to ∼2 nm. PA-BT-ODA showed the better exfoliation if take into account that low presence of monolayer structures remains after the compounding.

Transmission electron microscopy micrographs of the PA 6 nanocomposites are shown in Fig. 3. Most platelet thickness deduced from these photomicrographs is slightly higher than that of a single clay layer, indicating that organoclays are not fully exfoliated. In the TEM micrographs was not possible to distinguish the illite clay and the layered clay. However, an intercalated–exfoliated structure is observed,

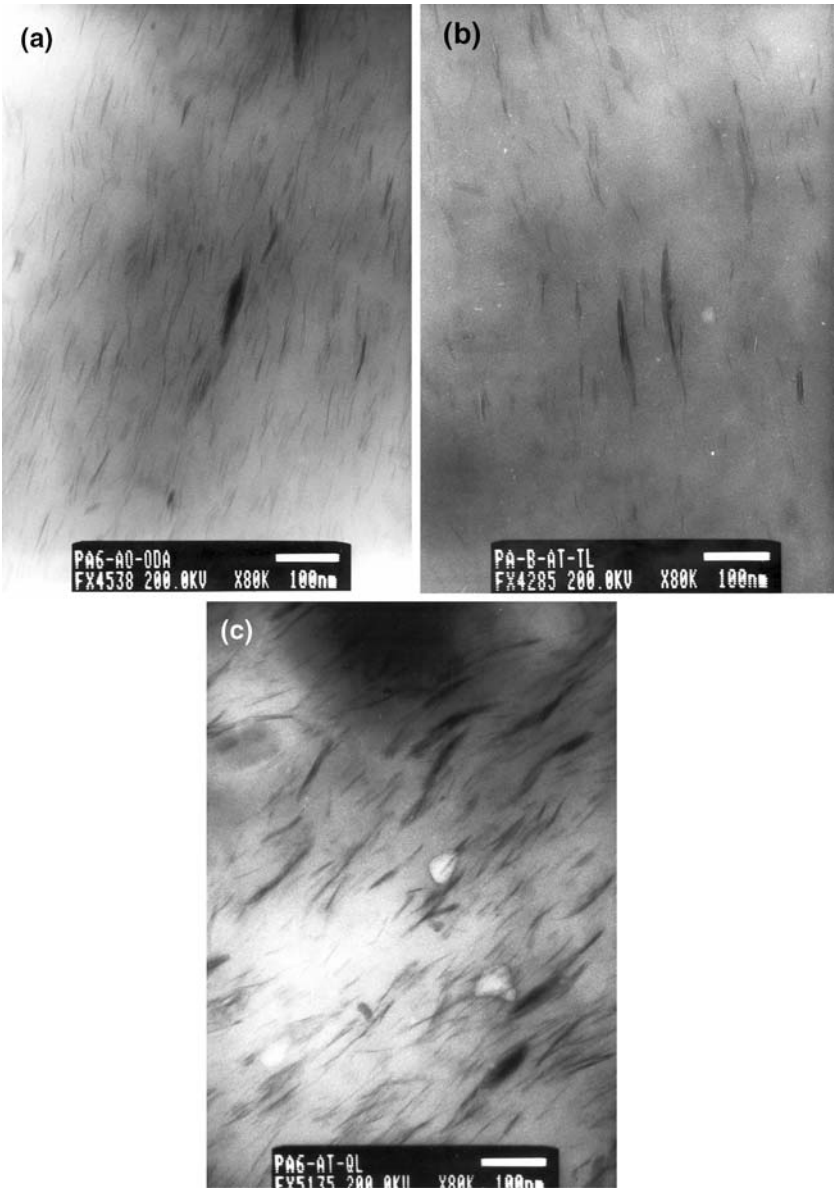

Fig. 3 TEM micrographs nanocomposites (×80,000) of: **a** PA 6-BT-ODA; **b** PA 6-BT-B2MTH; and **c** PA 6-BT-2M2TH

confirming XRD results. Organoclays became smaller and were dispersed more uniformly in PA 6-BT-ODA nanocomposite, in agreement with the XRD, showing an intercalated structure with a high level of exfoliated silicate layers. PA 6-BT-2M2TH nanocomposite presents a similar morphology but with a lower exfoliation grade, and an important amount of piled up platelets is observed. This

can be observed on the XRD results, where a peak at $2\theta = 5°$ is observed, corresponding to an intercalated structure of the clays. PA 6-BT-B2MTH nanocomposites show an intermediate behaviour that corresponds to the presence of two XRD peaks related with two different intergallery sizes; one of them corresponds to the structure of the modified clays and the other one to the intercalated structure produced during the extrusion process.

For PA 6-BT-2M2TH nanocomposite, it can be observed that the layers slide between them and resulting in an increase of the effective length [11]. The TEM evidences of this process are associated with the increasing of platelet length as well to the bifurcation and partial splitting of platelet stacks. This intercalated–exfoliated structure may be due to the fact that bentonite did not complete the cation exchange between the sodium cations and the organic modifier during the organoclay modification process as previously evidenced. Thus, the modifier located on the surface of the platelet stacks seems to restrain the intercalation of polymer and thus the exfoliation of the silicate layer because of their affinity with the polymer. In this sense, the organic modifier on the surface of the platelets stabilizes the platelet stacks and the organic modifier that is effectively incorporated into the clay galleries promotes the sliding between silicates layers resulting in deformable intercalates. In addition, there is some white type phase forming irregular form with smooth contour and nanosize in Fig. 3b and c that could also be attributed to free modifier. Such phase is organic in nature as confirmed by EDX and their absence in the PA-BT-ODA nanocomposite probes that neither is related to TEM sample procedure neither appeared in nanocomposites with most of the modifier located in the clays galleries.

Tensile modulus, HDT and Notched Izod impact strength values of PA6 and PA 6-organoclay nanocomposites are shown in Table 2. It can be observed that the presence of organoclays leads to substantial improvement in stiffness and heat deflection temperature (HDT), which correlated with a reduction in Izod impact strength in all PA 6 nanocomposites. Higher increases are obtained for both PA 6-BT-2M2TH and PA 6-BT-ODA nanocomposites (54% in tensile modulus and $\sim$35% in HDT) in comparison with PA-BT-B2MTH. It is interesting to remark that similar tensile modulus was observed for pure montmorillonite type organoclays [8] and the only difference was found in the HDT values. Previously, it was concluded that the presence of free modifier contributed to decrease only HDT parameter [8], but this contribution is slight. In such a case difference in clay platelet aspect ratio

Table 2 Properties of PA 6 nanocomposites

Sample	Clay treatment	Clay (wt%)	TGA clay content (wt%)	Tensile modulus (MPa)	HDT (°C)	Notched izod impact strength (kJ/m^2)
PA	–	–	–	2,637	48	6.67
PA 6-BT-ODA	5% solid spray dried + milling	5	3.4	4,060	66	3.84
PA 6-BT-B2MTH		5	4.0	3,893	62	4.16
PA 6-BT-2M2TH		5	3.5	4,000	66	4.82

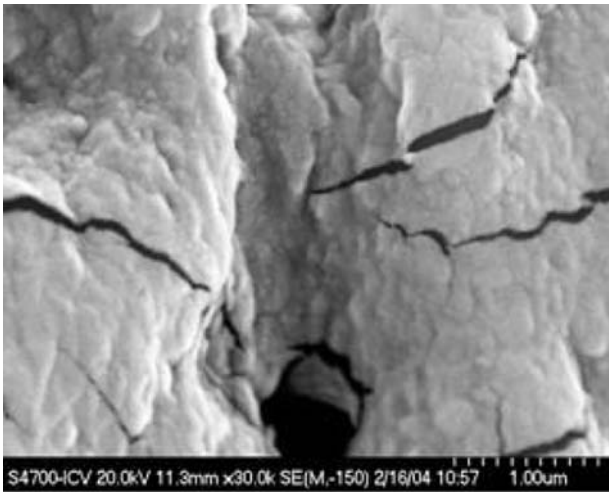

Fig. 4 FESEM micrograph of fresh nanocomposite fracture of PA 6-BT-2M2TH

could be contribute as well. So the question that arises at that point is as follow: are there different mechanisms that contributed to mechanical reinforcement of polymer/clay nanocomposites? Maybe the answer is quite complex and out of this paper but the experimental results obtained stated that probably more mechanisms than the inorganic-polymer interphase reinforcement could be involved. This mechanism was supported by the fact that this interphase produces a higher thermal stability of the nanocomposites, that is the polymer-inorganic interphase stiffness the polymer. Two possible contributions could appointed: (a) crack deflection due to presence of inorganic nanofiller as shown in micrograph of Fig. 4. The inorganic particles with higher module than the matrix acted as crack energy adsorption and produce an enhancement of the crack tortuosity. This mechanism is more efficient when the inorganic particles are under compressive stress as evidence with the presence of bridges at the tip of the crack. This type of fracture behaviour occurs in the different nanocomposites studies and is quite different than the more cohesive fracture behaviour usually observed in pure PA6 polymers. (b) The higher aspect ratio of deformed intercalates in samples with low R_{gem} ratios due in part to higher flexibility of this nanostructures. The higher dispersion of the layered silicates were translated to lower values of the Izod impact strength for the PA 6-BT-ODA nanocomposites indicating higher rigidity of the structure. The differentiation of the proposed possible mechanism is thus quite difficult because all samples shown similar tensile modulus and all of them could contribute simultaneously. The presence of intercalated structures seems to be on the base of proposed mechanisms.

Conclusions

An intercalated–exfoliated structure has been evidenced by XRD and TEM analysis for PA 6 nanocomposites formed with bentonites modified with ODA, 2M2TH and

B2MTH modifiers. The chemical structure of the organic modifier used for bentonite treatment, related to its thermal stability and its ability to penetrate into the clay galleries has a meaningful influence on organoclay exfoliation. However, the similarities on mechanical properties of PA 6 nanocomposites stated that a different mechanism could be taken into account. A possible crack deflection mechanism based on nanofiller presence was observed in PA6/organobentonite nanocomposite.

Acknowledgments This work is supported by the Ministerio de Educación y Ciencia [program MAT2007-66845-C02-01, Program MAT2005-06627-C03 and the European Social Foundation (ESF) Torres Quevedo Program].

References

1. Zanetti M, Lomakin S, Camino G (2000) Macromol Mater Eng 279:1–9
2. Fornes TD, Yoon PJ, Hunter DL, Keskkula H, Paul DR (2002) Polymer 43:5915–5933
3. Fornes TD, Hunter DL, Paul DR (2003) Macromolecules 37:1793–1798
4. Limpanart S, Khunthon S, Taepaiboon P, Supaphol P, Srikhirin T, Udomkichdecha W, Boontongkong Y (2005) Mater Lett 59:2292–2295
5. Usuki A, Kojima Y, Kawasumi M, Okada A, Fukushima Y, Kurauchi T, Kamigaito O (1993) J Mater Res 8:1179–1184
6. Lan T, Pinnavaia TJ (1994) Chem Mater 6:2216–2219
7. Giannelis EP (1996) Adv Mater 8:29–35
8. García-López D, Gobernado-Mitre I, Fernández JF, Merino JC, Pastor JM (2005) Polymer 46(8):2758–2765
9. Lagaly G (1986) Solid State Ion 22:43–51
10. Lee SY, Kim SJ (2002) J Colloid Interf Sci 248:231–238
11. Fornes TD, Yoon PJ, Keskkula H, Paul DR (2001) Polymer 42:9929–9940